

that can be inscribed in a polygonal domain Q consisting of n points and line segments. This problem has been considered fairly well in computational geometry community for many years. See Chapter 50 of the Handbook of Discrete and Computational Geometry [12].

The earliest result was perhaps the SoCG'89 paper by Chew and Kedem [7]. They considered the problem and gave an incremental technique for handling all the combinatorial changes to the Delaunay triangulation of the polygonal domain Q under the distance function induced by the input polygon P while P is rotating. They gave an upper bound $O(k^4 n \lambda_4(kn))$ on the combinatorial changes, that is, the number of *critical orientations*, together with a deterministic $O(k^4 n \lambda_4(kn) \log n)$ -time algorithm, where $\lambda_s(n)$ the length of the longest Davenport–Schinzel sequence of order s including n distinct symbols. A few years later, the bound was improved to $O(k^4 n \lambda_3(n))$ by them, and thus the running time of the algorithm became $O(k^4 n \lambda_3(n) \log n)$ [8].

Toledo [21], and Sharir and Toledo [19] studied this problem (they called this problem *the extremal polygon containment problem*) and applied the motion-planning algorithm [14] to solve this problem. They gave an algorithm with running time $O(k^2 n \lambda_4(kn) \log^3(kn) \log \log(kn))$ that uses the parametric search technique of Megiddo [17].

These two results, $O(k^4 n \lambda_3(n) \log n)$ and $O(k^2 n \lambda_4(kn) \log^3(kn) \log \log(kn))$, are comparable to each other. The latter one implies a better time bound for large k ($k > n$) while the former one implies a better time bound for small k .

There was a randomized algorithm by Agarwal et al. [2] that finds a largest similar copy in $O(kn \lambda_6(kn) \log^3(kn) \log^2 n)$ expected time using parametric search technique of Megiddo [17]. The problem was also considered for special cases. Agarwal et al. [1] considered the problem of finding largest similar copy of a given convex k -gon with contained in a convex n -gon and gave an $O(kn^2 \log n)$ -time algorithm. Very recently, there were results on two variants. Bae and Yoon [5] gave an $O(n^2 \log n)$ -time algorithm for finding a largest empty square among a set of n points in the plane. Lee et al. [15] gave an algorithm for finding a largest triangle with fixed interior angles in a simple polygon with n vertices in $O(n^2 \log n)$ time.

However, no improvement to the worst-case time bounds by Chew and Kedem, and Sharir and Toledo has been known for the polygon placement problem.

New result. We make progress of improving the upper bound on the combinatorial changes considered during the rotation and the algorithm to compute a largest similar copy. We present an upper bound $O(k^2 n^2 \lambda_4(k))$ on the combinatorial changes, and this directly improves the time bound for the algorithm to $O(k^2 n^2 \lambda_4(k) \log n)$. This improves the previously best known results by Chew and Kedem [8] and Sharir and Toledo [19] in more than 25 years.

Compared to the combinatorial upper bound $O(k^4 n \lambda_3(n))$ by Chew and Kedem, our bound is smaller than their bound asymptotically for both k and n . Since $\lambda_4(k) = o(k \log^* k)$ [20] and $\lambda_3(n) = \Theta(n \alpha(n))$, our bound is $o(k^3 n^2 \log^* k)$ while their bound is $O(k^4 n^2 \alpha(n))$. Therefore, our algorithm outperforms theirs. Compared to the time bound $O(k^2 n \lambda_4(kn) \log^3(kn) \log \log(kn))$ by Sharir and Toledo [19], our running time outperforms theirs for both k and n without resorting to parametric search technique, because $n \lambda_4(k) \log n = o(\lambda_4(kn) \log^3(kn) \log \log(kn))$.

Thus our result improves the best result for the problem introduced in Chapter 50 of the Handbook of Discrete and Computational Geometry [12], and the result could be a stepping stone to closing the problem.

Overview of techniques. We achieve the improved upper bound by carefully analyzing the combinatorial changes in the edge Delaunay triangulation of Q (to be defined later, shortly eDT) while rotating P and by reducing the candidate size to consider for the changes. Following the approach of Chew and Kedem [8], our strategy consists of two parts: Counting the combinatorial changes in eDT for a constant k , and then counting the combinatorial changes with respect to k .

1. In the first part, we analyze the combinatorial changes for a fixed k . We consider a family of functions defined for each vertex and edge of P and compute their lower envelope. Since there are $O(k)$ vertices and edges of P , we compute $O(k)$ lower envelopes. We show that the complexity of each lower envelope is $O(n)$. Then we compute the breakpoints on the lower envelope of the $O(k)$ lower envelopes. To bound the number of combinatorial changes in eDT, we consider a placement of a scaled copy of P such that a vertex of Q and a vertex of P are in contact, which we call a *hinge*, and show that the number of breakpoints on the lower envelope defined for each hinge is $O(n)$. Since there are $O(n)$ hinges for a constant k , the number of combinatorial changes in eDT for θ increasing from 0 to 2π is $O(n^2)$.
2. In the second part, we analyze the combinatorial changes to eDT with respect to k . A combinatorial change to eDT corresponds to a quadruplet of pairs, each pair consisting of an element of Q and an element of P touching each other in some placement of a scaled copy of P simultaneously. To count the quadruplets inducing combinatorial changes to eDT, we consider the triplets of such pairs and define a function for each triplet implying the size of the scaled copy of P defined by the triplet, satisfying the followings: For the lower envelope L of the functions, a combinatorial change corresponds to an intersection of two such functions appearing on L . That is, every combinatorial change to eDT occurs at a breakpoint on the lower envelope of the functions. So, the complexity of the lower envelope bounds the number of combinatorial changes that occur during the rotation of P . We reduce the complexity bound on the lower envelope by classifying the combination of pairs for the quadruplets.

While this high-level strategy may appear similar to the previous one [8], there are a few major differences and difficulties in improving the bound. In the first part, we improve the previous bound $O(n\lambda_3(n))$ by Chew and Kedem as follows. We partition the family of functions to subfamilies such that the functions in the same subfamily have the same domain length, and therefore the complexity of their lower envelope becomes linear to the number of functions [5, 15]. Thus, the total upper bound is improved to $O(n^2)$.

In the second part, instead of the quadruplets considered by Chew and Kedem, we consider the triplets of pairs only and show that the functions for the triplets, in their lower envelope, give us an upper bound on the number of the combinatorial changes to eDT. These functions must reflect the placement of a scaled copy of P that can be inscribed in Q as well as the scaling factor. We present a function definition satisfying this requirement and show that every combinatorial change to eDT occurs at a breakpoint on the lower envelope of the functions. There are $O(k^3n^2)$ such functions and two functions intersect at most four times. Thus, the complexity of the lower envelope of the functions is $O(\lambda_6(k^3n^2))$ as the lower envelope corresponds to a Davenport-Schinzel sequence of order 6. To reduce the bound, we classify the functions into types based on the combinations of pairs defining the functions and show that any two functions belonging to the same type intersect each other less than four times. By applying the partition method in the first part and the classification above on the functions, we show that the complexity of the lower envelope becomes $O(k^2n^2\lambda_4(k))$.

Due to the limit of space, the proofs of some lemmas and corollaries are given in Appendix.

2 Preliminary

2.1 Davenport–Schinzel sequences and lower envelopes

A Davenport–Schinzel sequence is a sequence of symbols in which the frequency of any two symbols appearing in alternation is limited. We call a Davenport–Schinzel sequence of order

s that includes n distinct symbols a DS(n, s)-sequence, and denote by $\lambda_s(n)$ the length of the longest DS(n, s)-sequence. For a DS(n, s)-sequence U , let $U(j)$ denote the j -th entry of U . We say a symbol a_i of U is *active* at j if $U(j') = a_i$ and $U(j'') = a_i$ for some $j' \leq j$ and $j'' > j$. Let $\nu(j)$ denote the number of active symbols of U at j . We say U is a DS(n, s, m)-sequence if $\nu(j) \leq m$ for each j . We denote by $\lambda_{s,m}(n)$ the length of the longest DS(n, s, m)-sequence.

We use some properties and lemmas related to Davenport–Schinzel sequences in analyzing algorithms. Let $\mathcal{F} = \{f_1, \dots, f_n\}$ be a collection of n partially-defined, continuous, one-variable real-valued functions. The points at which two functions intersect in their graphs and endpoints of function graphs are called the *breakpoints*. If any two functions f_i and f_j intersect in their graphs at most s times, the lower envelope of \mathcal{F} has at most $\lambda_{s+2}(n)$ breakpoints [3]. We introduce some technical lemmas that are used in Section 3.

Lemma 1 (Lemma 14 of [15]). *Assume any two functions f_i and f_j intersect in their graphs at most once and each function f_i has domain D_i of length d . If there is a constant c such that $|\bigcup D_i| = cd$, then the lower envelope of \mathcal{F} has $O(n)$ breakpoints.*

Proof. Let $D_{\mathcal{F}}$ be the union of all D_i 's. Let l_i be the point of $D_{\mathcal{F}}$ at distance di from the leftmost point of $D_{\mathcal{F}}$, for $i = 0, 1, \dots, \lceil c \rceil$. Then $l_j < l_{j'}$ for any two indices $0 \leq j < j' \leq \lceil c \rceil$. Then these points l_i 's partition $D_{\mathcal{F}}$ into intervals such that each interval has length d , except the last one of length smaller than or equal to d . Observe that each D_i intersects at most two consecutive intervals.

Let $L(j) = \{f_i|_{[l_{j-1}, l_j]} \mid l_j \in D_i\}$ and $R(j) = \{f_i|_{[l_j, l_{j+1}]} \mid l_j \in D_i\}$ be the sets of functions defined on the intervals with $0 < j < \lceil c \rceil$. Since any two functions in $L(j)$ intersect in their graphs at most once and their domains have l_j as the right endpoint, the lower envelope of $L(j)$ forms a Davenport–Schinzel sequence of order 2, and therefore the lower envelope of $L(j)$ has complexity $O(|L(j)|)$. Similarly, the lower envelope of $R(j)$ has complexity $O(|R(j)|)$. Since the union U_L of all $L(j)$'s and the union U_R of all $R(j)$'s have $O(n)$ functions, the lower envelope of each union has complexity $O(n)$.

Now, consider a new partition of $D_{\mathcal{F}}$ obtained by slicing it at every breakpoint on the lower envelopes of U_L and U_R . Since there are $O(n)$ such breakpoints and the lower envelope of \mathcal{F} restricted to a component of the new partition has a constant complexity, the complexity of the lower envelope of \mathcal{F} is $O(n)$. \square

Lemma 2 (Lemma 1 of [13]). *$\lambda_{s,m}(n)$ is $O(\frac{n}{m}\lambda_s(m))$.*

Corollary 3. *Let $\mathcal{G} = \{g_1, \dots, g_m\}$ be a collection of m partially-defined, piecewise continuous, one-variable real-valued functions. Let n be the total number of continuous pieces in the function graphs of \mathcal{G} . If any pair of continuous pieces intersect in at most s points, the lower envelope of \mathcal{G} has $O(\frac{n}{m}\lambda_{s+2}(m))$ breakpoints.*

Proof. Let $\mathcal{G}' = \{g'_1, \dots, g'_n\}$ be the set of all continuous pieces in \mathcal{G} . Let I_1, \dots, I_l be the interior-disjoint intervals induced by the breakpoints of lower envelope of \mathcal{G}' , such that I_j lies to the left of $I_{j'}$ if $j < j'$ for any two indices j and j' . Note that the set of intervals I_1, \dots, I_l is a partition of the domain of \mathcal{G} . Then the lower envelope of \mathcal{G} restricted to interval I_j consists of exactly one continuous piece of \mathcal{G}' . Let u_j be the index of the continuous piece appearing in the lower envelope in I_j . Then $U = \langle u_1, \dots, u_l \rangle$ is the sequence representing the lower envelope of \mathcal{G} . Since the number of active symbols at any position of the domain of \mathcal{G} is at most one, U is a DS($n, s + 2, m$)-sequence. Therefore, the lower envelope of \mathcal{G} has $O(\frac{n}{m}\lambda_{s+2}(m))$ breakpoints by Lemma 2. \square

2.2 Edge Voronoi diagrams and edge Delaunay triangulations

We introduce the *edge Voronoi diagram* and its dual, the *edge Delaunay triangulation* (eDT), which are described in [8]. The set S of sites consists of the edges (open line segments) and their endpoints in the polygonal domain Q of size n . For a convex polygon P with k vertices, the P -distance from a point p to a point q is $d_P(p, q) = \inf\{\mu | q \in p + \mu P\}$. The Voronoi diagram is a subdivision of the plane into regions such that the points in the same region all have the same nearest site under the P -distance. See Figure 1(a).

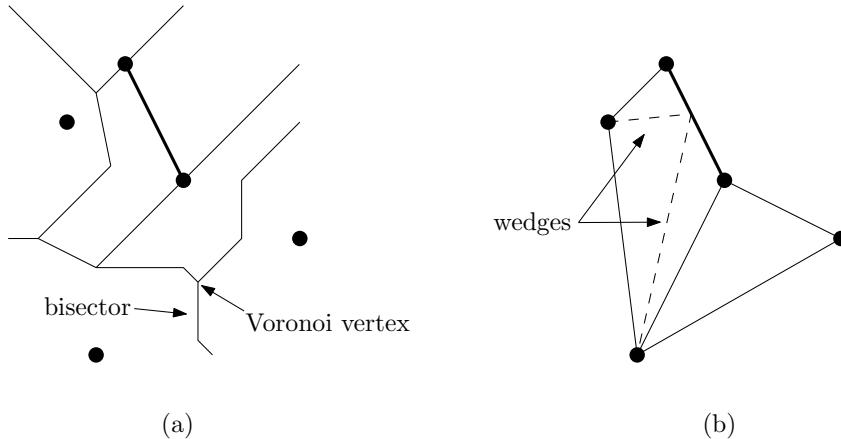


Figure 1: (a) The edge Voronoi diagram of sites under P -distance when P is an axis-aligned square. (b) The edge Delaunay triangulation dual to the edge Voronoi diagram in (a).

The edge Voronoi diagram consists of *Voronoi vertices* and *Voronoi edges (bisectors)*. A point in the plane is a Voronoi vertex if and only if there is an empty circle defined by the P -distance centered at the point and touching three or more sites. It is known that the number of Voronoi vertices is linear to the complexity of the sites [11]. The bisector between two sites defines a Voronoi edge if and only if there is an empty circle defined by the P -distance centered at a point on the bisector and touching the sites. A Voronoi edge is a polygonal line that connects two adjacent Voronoi vertices and each point on the edge is equidistant from the two sites defining the edge under the P -distance. The edge Voronoi diagram can be built in $O(kn \log kn)$ time and $O(kn)$ space.

Just as the standard Delaunay triangulation is the dual of the standard Voronoi diagram, the edge Delaunay triangulation (eDT) is the dual of the edge Voronoi diagram. It has three types of *generalized edges*: *edges*, *wedges*, and *ledges*. An edge connects two point sites, a wedge connects a point site and a segment site, and a ledge connects two segment sites. See Figure 1(b). The edge Delaunay triangulation is a planar graph consisting of point sites, segment sites, generalized edges, and empty triangles. Since a ledge is a trapezoid or a degenerate trapezoid, eDT is actually not a true triangulation in general.

The edge Delaunay triangulation can be constructed by first building the edge Voronoi diagram and then tracing the diagram to determine the sites that define each portion of the Voronoi edges and vertices. The type of a generalized edge is determined by the sites defining the corresponding Voronoi edge.

An ordered pair (A, B) is a *side contact pair* if A is a side of Q and B is a corner of P , and a *corner contact pair* if A is a corner of Q and B is a side of P . A side contact pair or a corner contact pair is called a *contact pair*. We denote by \mathcal{P} a homothetic copy of P . We say \mathcal{P} *satisfies* a contact pair (A, B) if B in \mathcal{P} touches A . See Figure 2. We say \mathcal{P} is *feasible* if \mathcal{P} is inscribed in

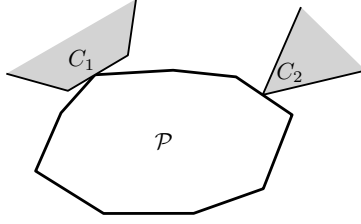


Figure 2: \mathcal{P} satisfies a side contact pair C_1 and a corner contact pair C_2 .

Q . Note that \mathcal{P} is not necessarily feasible even if \mathcal{P} satisfies a contact pair.

2.3 The Algorithm of Chew and Kedem

We introduce the algorithm by Chew and Kedem. Imagine we rotate P by angle θ in counter-clockwise direction. Let P_θ be the rotated copy of P , and let \mathcal{P}_θ be a homothetic copy of P_θ . Let eDT_θ denote the edge Delaunay triangulation of the sites in S with respect to the P_θ -distance. For a face T of eDT_θ , we say a \mathcal{P}_θ is associated to T if it touches all the sites defining T . For \mathcal{P}_θ associated to T , the set of the elements (vertices or edges) of \mathcal{P}_θ touching the sites defining T becomes the label of T . See Figure 3(a). For a site s of S , the label of s is the set of elements of \mathcal{P}_θ 's touching s , for \mathcal{P}_θ 's associated to the faces incident to s . See Figure 3(b).

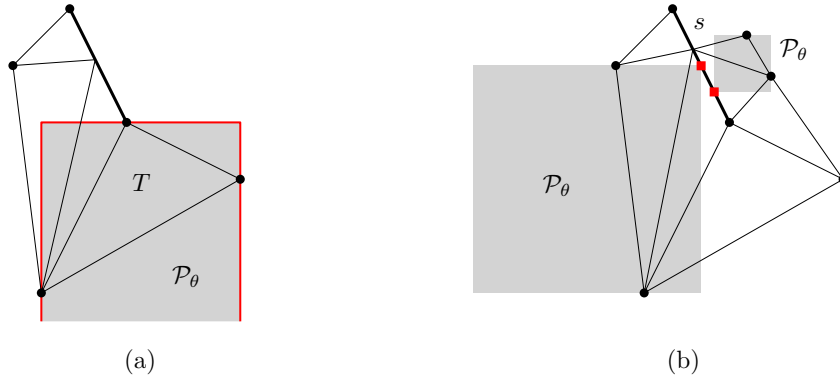


Figure 3: Labels of faces of eDT_θ and edge sites of S for an axis-aligned square P_θ . (a) The label of face T is the set of red edges of \mathcal{P}_θ . (b) The label of edge site s is the set of red corners of \mathcal{P}_θ 's.

Their algorithm classifies two possible types of changes, an edge change and a label change in eDT_θ while θ increases. In an edge change, a new generalized edge appears or an existing edge disappears. This change occurs when \mathcal{P}_θ touches four elements of Q , resulting in a flip of the diagonals in the quadrilateral formed by the four edges of eDT_θ . In a label change, the label of a face in eDT_θ changes. This occurs when two or more elements of \mathcal{P}_θ touch the same site, but the structure of eDT_θ may be unchanged. An edge change or a label change is called a *combinatorial change* to eDT_θ .

Their algorithm constructs and maintains a representation for eDT_θ while θ increases. It starts by creating eDT_θ at $\theta = 0$. For each generalized edge in eDT_θ , it determines at which orientation this edge ceases to be valid due to an interaction with its neighbors. For each face in eDT_θ , the algorithm determines at which orientation the label of this face changes. An edge change is detected by checking the edges of eDT_θ and a label change is detected by checking

the faces of eDT_θ . The algorithm maintains the edges and faces of eDT_θ in a priority queue, ordered by the orientations at which they are changed. At each succeeding stage of the algorithm, it determines which generalized edge is the next one to disappear or which face has its label changed as θ increases. Then, it updates eDT_θ and the priority queue information for the new edge and its neighbors. Note that a new edge may change the priority for its neighbors. A priority queue can be implemented such that each operation can be done $O(\log m)$ time, where m is the maximum number of items in the queue. Since there are never more than $O(n)$ edges and faces in the queue at any one time, each priority queue operation takes time $O(\log n)$.

For each event of a face T disappearing at θ_e , the algorithm finds the maximal interval $\mathcal{I} = [\theta_s, \theta_e]$ of θ such that T appears on eDT_θ . To find \mathcal{I} in $O(1)$ time, it stores at T the orientation at which it starts to appear on eDT_θ . Then it computes the orientation $\theta^* \in \mathcal{I}$ that maximizes the area of each \mathcal{P}_θ that satisfies the contacts induced by T . Since \mathcal{I} is the maximal interval, \mathcal{P}_θ is feasible for every $\theta \in \mathcal{I}$ but not for any $\theta \notin \mathcal{I}$ sufficiently close to \mathcal{I} . Thus, the algorithm considers all orientations that \mathcal{P}_θ is feasible and computes the placement and orientation of the largest similar copy of P . Note that the area function of \mathcal{P}_θ can be computed in $O(1)$ time and the number of \mathcal{P}_θ that satisfies the contacts induced by T is $O(1)$. Chew and Kedem gave an upper bound $O(k^4 n \lambda_3(n))$ on the combinatorial changes, and their algorithm takes $O(k^4 n \lambda_3(n) \log n)$ time [8].

3 The number of changes in eDT_θ

We show that the number of combinatorial changes during the rotation is $O(k^2 n^2 \lambda_4(k))$ in this section. This directly improves the time bound for the algorithm to $O(k^2 n^2 \lambda_4(k) \log n)$. We analyze the number of combinatorial changes in eDT_θ for a constant k in Section 3.1, and then analyze the number of combinatorial changes with respect to k in Section 3.2 using the observation in Section 3.1. We use the reference point (x, y) , the reference orientation θ , and the expansion factor δ of \mathcal{P}_θ defined in [8], which represent a placement of \mathcal{P}_θ in the plane by a quadruplet (x, y, θ, δ) .

3.1 The number of changes for fixed k

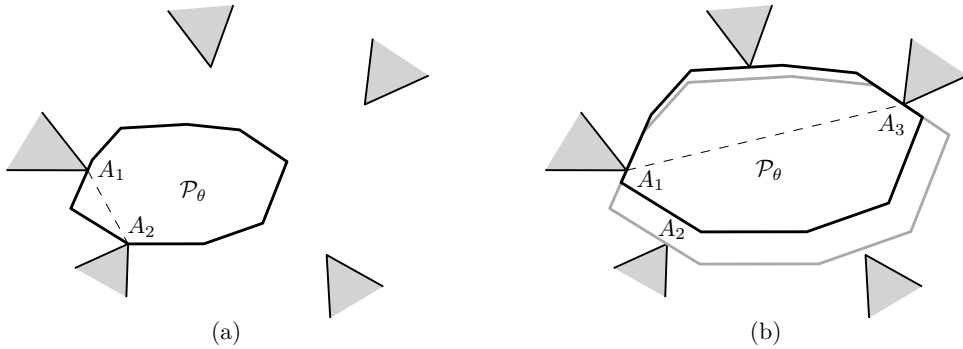


Figure 4: (a) The segment A_1A_2 is a reported edge with $Q_H = A_2$. (b) The segment A_1A_3 is an unreported edge because no hinge is involved in the segment for a feasible \mathcal{P}_θ .

For a constant k , we improve the previously best upper bound $O(n \lambda_3(n))$ by Chew and Kedem [8] to $O(n^2)$. A key idea is to consider the lower envelope of some functions related to the expansion factor, one for each edge and vertex of P , and then to analyze the lower envelope

of those lower envelopes. By careful analysis on the complexities of the lower envelopes, we show that the number of combinatorial changes to eDT_θ for θ increasing from 0 to 2π is $O(n^2)$.

An ordered pair (Q_H, P_H) is a *hinge* if Q_H is a corner of Q and P_H is a corner of P . For a hinge $H = (Q_H, P_H)$ and a contact pair $C = (A, B)$, the generalized edge connecting Q_H and A is a *reported edge* if there is a feasible \mathcal{P}_θ for some θ satisfying both H and C . An edge of eDT_θ is an *unreported edge* if it is not a reported edge. See Figure 4.

Changes to the reported edges and the label changes to point sites. We count the changes to the reported edges and the changes to the labels of point sites in eDT_θ for θ increasing from 0 to 2π . We define the *expansion function* $E_{HC}(\theta)$ for a hinge H and a contact C to be the minimal expansion factor of \mathcal{P}_θ satisfying H and C . For a hinge $H = (Q_H, P_H)$, let \mathcal{F}_H be the set of all expansion functions satisfying H and another contact pair. An expansion function $E_{HC}(\theta)$ of \mathcal{F}_H for a contact $C = (A, B)$ appears on the lower envelope of \mathcal{F}_H at θ if the generalized edge connecting Q_H and A is a reported edge in eDT_θ . Then the number of changes to the reported edges in eDT_θ which involve H is bounded by the number of breakpoints on the lower envelope of \mathcal{F}_H .

Every label change to a point site involves a hinge. See Figure 5(a). An intersection of E_{HC_1} and E_{HC_2} of \mathcal{F}_H for contact pairs C_1 and C_2 appears on the lower envelope of \mathcal{F}_H if a label change to a point site is induced by C_1, C_2 and H . Then the number of label changes to the point sites in eDT_θ which involve H is bounded by the number of breakpoints on the lower envelope of \mathcal{F}_H .

Proposition 4 (Proposition 3 of [8]). *Two expansion functions E_{HC_1} and E_{HC_2} intersect each other in at most one point in their graphs if both C_1 and C_2 are corner contact pairs, or both are side contact pairs. If one is a corner contact pair and the other is a side contact pair, E_{HC_1} and E_{HC_2} intersect in at most two points in their graphs.*

Let v_i and e_i denote the vertices and edges of P for $i = 1, \dots, k$. For each $i = 1 \dots k$, let $\mathcal{C}_{1i} = \{(e, v_i) \mid e \text{ is an edge of } Q\}$ be the set of side contact pairs and let $\mathcal{C}_{2i} = \{(v, e_i) \mid v \text{ is a vertex of } Q\}$ be the set of corner contact pairs. Let $\mathcal{F}_{ji} = \{E_{HC} \mid C \in \mathcal{C}_{ji}\}$ for $j = 1, 2$.

Lemma 5. *The number of breakpoints on the lower envelope of \mathcal{F}_{ji} is $O(n)$ for each $j = 1, 2$ and $i = 1, \dots, k$.*

Proof. The number of breakpoints on the lower envelope of \mathcal{F}_{1i} is $O(n)$ for each i since E_{HC_1} and E_{HC_2} intersect only at the boundaries of their intervals for $C_1, C_2 \in \mathcal{C}_{1i}$.

Consider now the number of breakpoints on the lower envelope of \mathcal{F}_{2i} . Two expansion functions E_{HC_1} and E_{HC_2} intersect in at most one point for $C_1, C_2 \in \mathcal{C}_{2i}$. Also, E_{HC} has the same length of domain for all $C \in \mathcal{C}_{2i}$. Thus, the number of breakpoints on the lower envelope of \mathcal{F}_{2i} is $O(n)$ by Lemma 1. \square

From Corollary 3, Proposition 4, and Lemma 5, we achieve an upper bound on the number of breakpoints on the lower envelope of \mathcal{F}_H .

Lemma 6. *The number of breakpoints on the lower envelope of \mathcal{F}_H is $O(\lambda_3(k)n)$.*

Proof. Let $\mathcal{F}_j = \{f_{j1}, \dots, f_{jk}\}$ for $j = 1, 2$, where f_{ji} is the lower envelope of \mathcal{F}_{ji} for each $i = 1, \dots, k$ and $j = 1, 2$. Let \mathcal{L}_j denote the lower envelope of \mathcal{F}_j . Then, the lower envelope of \mathcal{F}_H is the lower envelope of \mathcal{L}_1 and \mathcal{L}_2 . The number of breakpoints on \mathcal{L}_j is $O(\lambda_3(k)n)$ for $j = 1, 2$ by Corollary 3, Proposition 4, and Lemma 5. The number of breakpoints on the lower envelope of \mathcal{F}_H is also $O(\lambda_3(k)n)$, because two continuous pieces, one from \mathcal{L}_1 and one from \mathcal{L}_2 , intersect at most two points by Proposition 4. \square

By Lemma 6, the number of changes to the reported edges and the number of label changes to the point sites are $O(k\lambda_3(k)n^2)$.

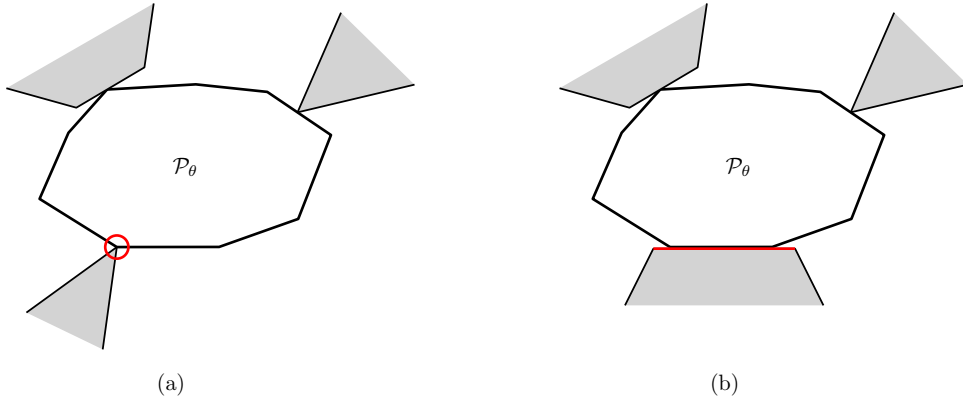


Figure 5: The label changes to the red sites. (a) Label change to a point site (hinge). (b) Label change to an edge site.

Label changes to edge sites. We count the changes to the labels of edge sites in eDT_θ for θ increasing from 0 to 2π . Imagine we fix an edge e of Q and an edge g of P . See Figure 5(b). Then, the number of label changes to edge site e with g is $O(n)$ because the edge site and the edge of P are aligned. The number of label changes to all edge sites is $O(kn^2)$.

Changes to unreported edges. We count the changes to unreported edges using the numbers of changes to the reported edges and to the labels, and Lemma 7.

Lemma 7 (Lemma 2 of [8]). *Every edge of eDT_θ is either a reported edge or a diagonal in a convex l -gon, $l \leq 3k$, whose sides are either reported edges or portions of edge sites.*

Let G_θ be the graph whose edges are the reported edges in eDT_θ and portions of edge sites in Lemma 7. We count the changes to the unreported edges which are diagonals in a face of G_θ for an interval of θ with no label change to eDT_θ . Observe that no combinatorial change occurs to G_θ for the interval. Any change to an unreported edge involves four sites lying on a face boundary of G_θ . There are at most four changes for a group of four sites. We describe the details on this bound in Section 4. Since each face has at most $3k$ edges by Lemma 7, there are at most $\binom{3k}{4}$ such groups. Since $O(k^4)$ changes occur to the unreported edges for the boundary of a face g of G_θ during an interval of θ with no label change to the faces of eDT_θ intersecting g , there are $O(k^5 n^2 \lambda_3(k))$ combinatorial changes to eDT_θ .

Theorem 8. *For a polygonal domain Q of size n and a convex k -gon P , the number of combinatorial changes to eDT_θ for θ increasing from 0 to 2π is $O(n^2)$ for a constant k .*

3.2 The number of changes with respect to k

We now consider k as a variable and bound the number of changes to eDT_θ . Since each triangular face in eDT_θ is defined by three elements (edges or vertices) of P , we choose three elements of P then use their convex hull in the counting. Then the number of faces in eDT_θ for all these convex hulls is at most $O(k^3 n^2)$ for θ increasing from 0 to 2π , by Theorem 8. Let \mathcal{T} be the set of all faces of eDT_θ for the convex hull P' for three elements B_1, B_2, B_3 of P such that the contact pairs inducing the face have B_1, B_2 , and B_3 as their elements.

Consider two faces T and T' of eDT_θ for two distinct orientations $\theta = \theta_1$ and $\theta = \theta_2$ with $\theta_1 < \theta_2$ that are defined by the same sites. We consider T and T' as distinct faces if there is any change to T or T' in eDT_θ for θ from θ_1 to θ_2 . For a face $T \in \mathcal{T}$, let $C(T)$ be the set of contact pairs which defines T , and let $I(T)$ be the interval of θ at which T appears to eDT_θ .

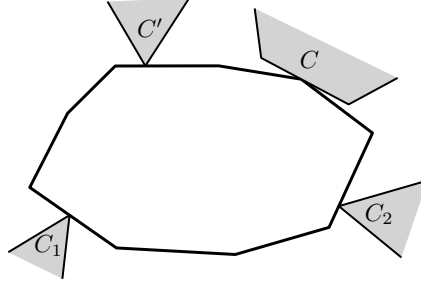


Figure 6: The combinatorial change induced by C_1, C_2, C , and C' .

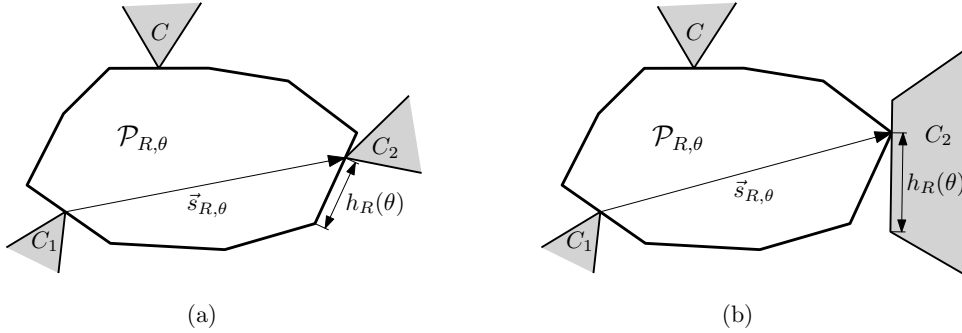


Figure 7: $\mathcal{P}_{R,\theta}$, $\vec{s}_{R,\theta}$, and $h_R(\theta)$ for a restricted contact pair $R = (C, I)$ and θ . Let $h_R(\theta)$ be the distance from the clockwise endpoint (with respect to $\vec{s}_{R,\theta}$) of the side element of C_2 to point element of C_2 . (a) $h_R(\theta)$ when C_2 is a corner contact. (b) $h_R(\theta)$ when C_2 is a side contact.

For any two fixed contact pairs (C_1, C_2) , we count the combinatorial changes involving (C_1, C_2) , and other contact pairs C and C' given in counterclockwise order C_1, C_2, C , and C' along the boundary of P . See Figure 6. Note that for (C_1, C_2) with $C_i = (A_i, B_i)$ for $i = 1, 2$, we do not count the combinatorial changes for the pair if $A_1 = A_2$ or $B_1 = B_2$. The combinatorial changes not counted are counted for other two fixed contact pairs.

We use (C, I) to denote a contact pair C restricted to an interval I of θ . Let \mathcal{R} be the set of *restricted contact pairs* (C, I) such that $C(T) = \{C_1, C_2, C\}$ and $I = I(T)$ for a face $T \in \mathcal{T}$, and C_1, C_2, C appear in counterclockwise order along P . For a fixed restricted contact pair $R \in \mathcal{R}$ and $\theta \in I$ for $R = (C, I)$, let $\mathcal{P}_{R,\theta}$ denote the homothet of P_θ which satisfies C_1, C_2 , and C . We use $\vec{s}_{R,\theta}$ to denote the ray from the point element of C_1 to the point element of C_2 in $\mathcal{P}_{R,\theta}$. Let $h_R(\theta)$ be the function that denotes the distance from the clockwise endpoint (with respect to $\vec{s}_{R,\theta}$) of the side element of C_2 to point element of C_2 with respect to $\mathcal{P}_{R,\theta}$. See Figure 7.

Observe that h_R is a partially defined continuous function on $R \in \mathcal{R}$. Let $\mathcal{F} = \{h_R \mid R \in \mathcal{R}\}$. Two restricted contact pairs $R, R' \in \mathcal{R}$ are in the same *class* if and only if there is a subset $\{f_1, \dots, f_j\} \subset \mathcal{F}$ with $f_1 = h_R, f_j = h_{R'}$ such that $f_{j'}$ and $f_{j'+1}$ intersect each other for every $j' = 1, \dots, j - 1$. Figure 8 illustrates the classes of \mathcal{R} .

If a combinatorial change is induced by C_1, C_2, C , and C' at θ , we have $h_R(\theta) = h_{R'}(\theta)$ for distinct restricted contact pairs $R = (C, I)$ and $R' = (C', I')$. See Figure 6. Let $\mathcal{R}' \subset \mathcal{R}$ be a

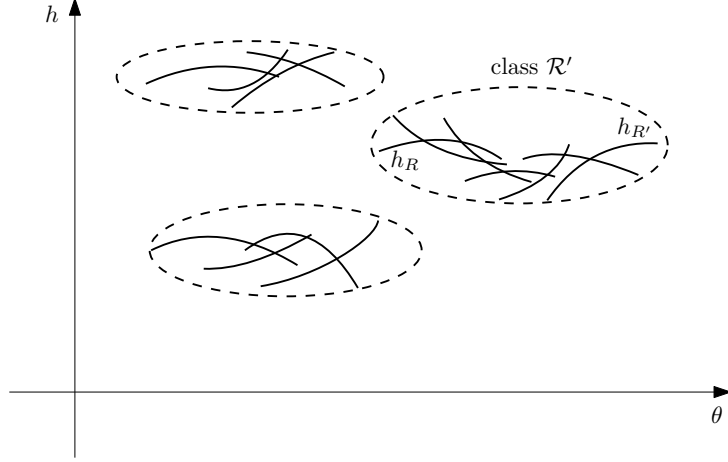


Figure 8: Partitioning \mathcal{R} by classes using the intersections of function graphs of \mathcal{F} . Class \mathcal{R}' has R and R' , and there is a sequence f_1, \dots, f_j with $f_1 = h_R, f_j = h_{R'}$ such that $f_{j'}$ and $f_{j'+1}$ intersect each other for every $j' = 1, \dots, j - 1$.

subclass of \mathcal{R} and let $\mathcal{F}' = \{h_R \mid R \in \mathcal{R}'\}$. We verify that if $\mathcal{P}_{R,\theta}$ is feasible, then $h_R(\theta)$ appears on the lower envelope or upper envelope of \mathcal{F}' .

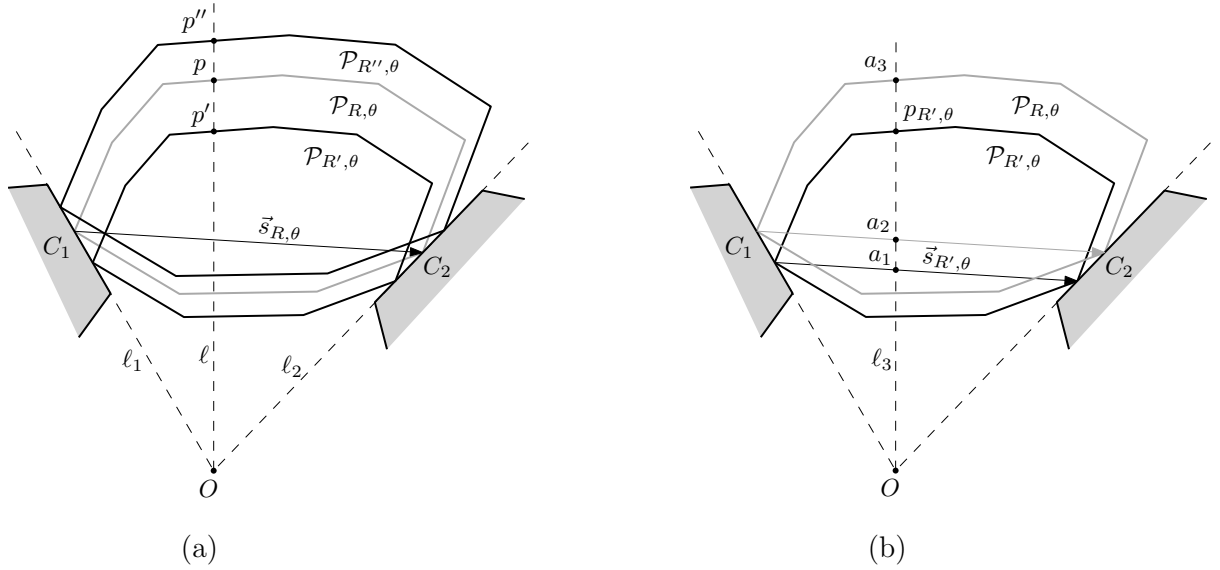


Figure 9: Proof of Lemma 9.

Lemma 9. *Let $R, R', R'' \in \mathcal{R}$ be the restricted contact pairs in the same class. If $h_{R'}(\theta) < h_R(\theta) < h_{R''}(\theta)$, then $\mathcal{P}_{R,\theta}$ is not feasible.*

Proof. Let $R = (C, I), R' = (C', I')$, and $R'' = (C'', I'')$. Let ℓ_1 be the line through the edge element of C_1 , ℓ_2 be the line through the edge element of C_2 , and O be the intersection of ℓ_1 and ℓ_2 unless they are parallel. For a fixed point \bar{p} on the boundary of P , let p', p , and p'' be the points on the boundaries of $\mathcal{P}_{R',\theta}, \mathcal{P}_{R,\theta}$, and $\mathcal{P}_{R'',\theta}$, respectively, corresponding to \bar{p} . Then p', p , and p'' are on the same line ℓ and the order of p', p , and p'' (with p in between p' and p'') on ℓ

remains the same for any choice of \bar{p} because $h_{R'}(\theta) < h_R(\theta) < h_{R''}(\theta)$. Observe that ℓ passes through O (if exists) and crosses both $\vec{s}_{R,\theta}$ and $\vec{s}_{R'',\theta}$. See Figure 9(a).

Let $p_{R',\theta}$ be the position of the point element of C' in $\mathcal{P}_{R',\theta}$. Let ℓ_3 be the line through O and $p_{R',\theta}$ if O exists. Otherwise, let ℓ_3 be the line through $p_{R',\theta}$ and parallel to ℓ_1 and ℓ_2 . Let $a_1 = \vec{s}_{R',\theta} \cap \ell_3$, $a_2 = \vec{s}_{R,\theta} \cap \ell_3$ and let a_3 be the point on the boundary of $\mathcal{P}_{R,\theta}$ corresponding to $p_{R',\theta}$ on $\mathcal{P}_{R',\theta}$. Without loss of generality, assume that ℓ_3 is vertical, and $p_{R',\theta}$ lies above a_1 .

Consider the case that $p_{R',\theta}$ lies below a_3 . See Figure 9(b). We show that $p_{R',\theta}$ does not lie on the segment a_1a_2 . Since R', R are in the same class, there is a subset $\{f_1, \dots, f_j\} \subset \mathcal{F}$ with $f_1 = h_{R'}$, $f_j = h_R$ such that $f_{j'}$ and $f_{j'+1}$ intersect each other for every $j' = 1, \dots, j-1$. Let $R_{j'} = (C_{j'}, I_{j'})$ be the restricted contact pair with angle interval $I_{j'}$ such that $h_{R_{j'}} = f_{j'}$ for $j' = 1, \dots, j$. Let $\mathcal{P}'_{R_{j'},\theta'}$ be the rotated and scaled copy of the convex hull of B_1, B_2 , and B' of $C_{j'} = (A', B')$, satisfying C_1, C_2 and $C_{j'}$. Then $\vec{s}_{R_{j'},\theta'}$ never intersects $p_{R',\theta}$ for any $\theta' \in I_{j'}$ and $j' = 1, \dots, j$ since $p_{R',\theta}$ does not lie in the interior of $\mathcal{P}'_{R_{j'},\theta'}$ but $\vec{s}_{R_{j'},\theta'}$ is contained in the interior of $\mathcal{P}'_{R_{j'},\theta'}$. Let $\theta_{j'} \in I_{j'}$ be one of the orientations at which an intersection of $f_{j'}$ and $f_{j'+1}$ occurs for each $j' = 1, \dots, j-1$. Then, $\vec{s}_{R_{j'},\theta_{j'-1}}$ can be translated continuously to $\vec{s}_{R_{j'},\theta_{j'}}$ for θ from $\theta_{j'-1}$ to $\theta_{j'}$ for each $j' = 2, \dots, j-1$. Also, $\vec{s}_{R',\theta}$ can be translated continuously to \vec{s}_{R',θ_1} , and $\vec{s}_{R,\theta_{j-1}}$ can be translated continuously to $\vec{s}_{R,\theta}$. If $p_{R',\theta}$ lies on a_1a_2 , $p_{R',\theta}$ lies on $\vec{s}_{R_{j'},\theta'}$ for some $j' = 1, \dots, j$ and $\theta' \in I_{j'}$. This contradicts to the fact that $\vec{s}_{R_{j'},\theta'}$ never intersects $p_{R',\theta}$. Thus, $p_{R',\theta}$ lies above a_1a_2 . Then $p_{R',\theta}$ lies in the interior of a_2a_3 , that is, $p_{R',\theta}$ lies in the interior of $\mathcal{P}_{R,\theta}$, and therefore $\mathcal{P}_{R,\theta}$ is not feasible.

Now consider the case that $p_{R',\theta}$ lies above a_3 . Then by an argument similar to the one for the previous case, we can show that $p_{R'',\theta}$ is contained in the interior of $\mathcal{P}_{R,\theta}$, where $p_{R'',\theta}$ is the position of the point element of C'' in $\mathcal{P}_{R'',\theta}$. Therefore $\mathcal{P}_{R,\theta}$ is not feasible. \square

Let \mathcal{R}'_{1i} be the subset of \mathcal{R}' such that $R = (C, I) \in \mathcal{R}'$ belongs to \mathcal{R}'_{1i} if $C = (e, v_i)$ is a side contact pair for some edge $e \in Q$. Let \mathcal{R}'_{2i} be the subset of \mathcal{R}' such that $R = (C, I) \in \mathcal{R}'$ belongs to \mathcal{R}'_{2i} if $C = (v, e_i)$ is a corner contact pair for some vertex $v \in Q$. Suppose that $|\mathcal{R}'| = m$ and $|\mathcal{R}'_{1i}| = m_{1i}, |\mathcal{R}'_{2i}| = m_{2i}$ for $i = 1, \dots, k$. Let $\mathcal{F}'_{ji} = \{h_R \mid R \in \mathcal{R}'_{ji}\}$ for $j = 1, 2$. First, we count the breakpoints on the lower envelope of \mathcal{F}'_{1i} and the lower envelope \mathcal{F}'_{2i} . The number of breakpoints on the lower envelope of \mathcal{F}'_{1i} is $O(m_{1i})$ since h_R and $h_{R'}$ can intersect only at the boundaries of their intervals for $R, R' \in \mathcal{R}'_{1i}$. Let d_i be the number of intersections of the function graphs of \mathcal{F}'_{2i} , and let $d = \sum_{i=1}^k d_i$. Then the number of breakpoints on the lower envelope of \mathcal{F}'_{2i} is $O(m_{2i} + d_i)$.

Lemma 10. *The number of breakpoints on the lower envelope of \mathcal{F}'_{1i} is $O(m_{1i})$ and \mathcal{F}'_{2i} is $O(m_{2i} + d_i)$ for each $i = 1, \dots, k$.*

Observe that each intersection of the function graphs of \mathcal{F}'_{2i} corresponds to a combinatorial change to eDT for the convex hull of B_1, B_2 , and e_i . See Figure 10. By Lemma 9, every combinatorial change appears on the lower envelope or upper envelope of \mathcal{F}' . Here, we describe the case for the lower envelope of \mathcal{F}' . We count the breakpoints of certain types on the lower envelope of \mathcal{F}' . The combinatorial changes corresponding to the breakpoints not counted here will be counted for other choices of the fixed pair. We use (a, b) -change to denote a combinatorial change induced by a side contact pairs and b corner contact pairs.

Two side contact pairs. We count only $(4, 0)$ -changes in this case. We count $(3, 1)$ and $(2, 2)$ -changes appearing on the lower envelope in other choices of the fixed pair. See Figure 11. By Corollary 3 and Lemma 10, the number of breakpoints on the lower envelope of $\mathcal{F}'_1 = \{f_i \mid i = 1, \dots, k\}$ is $\sum_{i=1}^k O(m_{1i}\lambda_4(k)/k) = O(m\lambda_4(k)/k)$, where f_i is the lower envelope of \mathcal{F}'_{1i} . In Section 4, we show that any two continuous pieces in \mathcal{F}'_1 intersect each other in at most two

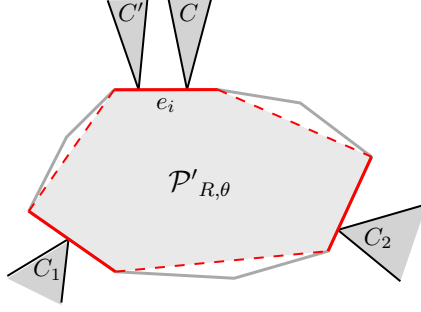


Figure 10: For $R = (C, I)$ and $R' = (C', I')$ in \mathcal{R}'_{2i} , and orientation θ with $h_R(\theta) = h_{R'}(\theta)$, there exists a rotated and scaled copy of the convex hull of B_1, B_2 , and e_i , satisfying C_1, C_2 and C, C' , and feasible. The intersection $h_R(\theta) = h_{R'}(\theta)$ corresponds to a combinatorial change to eDT_θ for the convex hull of B_1, B_2 , and e_i .

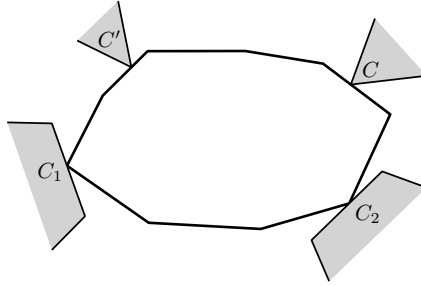


Figure 11: The $(2, 2)$ -change induced by C_1, C_2, C and C' is counted when C_2 and C are chosen as the fixed pair.

points. Since each $(4, 0)$ -change corresponds to a breakpoint on the lower envelope of \mathcal{F}'_1 , the number of $(4, 0)$ -changes is $O(m\lambda_4(k)/k)$.

Two corner contact pairs. We count only $(0, 4)$ -combinatorial changes in this case. Other changes are counted for other choices of the fixed pair. By Corollary 3 and Lemma 10, the number of breakpoints on the lower envelope of $\mathcal{F}'_2 = \{f_i \mid i = 1, \dots, k\}$ is $\sum_{i=1}^k O((m_{2i} + d_i)\lambda_4(k)/k) = O((m + d)\lambda_4(k)/k)$, where f_i is the lower envelope of \mathcal{F}'_{2i} . In Section 4, we show that any two continuous pieces in \mathcal{F}'_2 intersect each other in at most two points. Since each $(0, 4)$ -change corresponds to a breakpoint of the lower envelope of \mathcal{F}'_2 , the number of $(0, 4)$ -changes is $O((m + d)\lambda_4(k)/k)$.

One side contact pair and one corner contact pair. We count all combinatorial changes other than $(4, 0)$ -changes and $(0, 4)$ -changes. First, we count the breakpoints of the lower envelope of $\mathcal{F}'_1 = \{h_R \mid R \in \bigcup_{i=1}^k \mathcal{R}'_{1i}\}$ and of the lower envelope of $\mathcal{F}'_2 = \{h_R \mid R \in \bigcup_{i=1}^k \mathcal{R}'_{2i}\}$, then count the breakpoints of the lower envelope of $\mathcal{F}'_1 \cup \mathcal{F}'_2$. In Section 4, we show that any two continuous pieces, both from either \mathcal{F}'_1 or \mathcal{F}'_2 , intersect each other in at most two points. The number of breakpoints of the lower envelope of \mathcal{F}'_1 can be computed in the same way as for counting $(4, 0)$ -changes, and the result is $O(m\lambda_4(k)/k)$. The number of breakpoints of the lower envelope of \mathcal{F}'_2 can be computed in the same way as for counting $(0, 4)$ -changes, and the result is $O((m + d)\lambda_4(k)/k)$. The number of breakpoints of the lower envelope of \mathcal{F}' is $O((m + d)\lambda_4(k)/k)$, since the number of breakpoints of the lower envelope of \mathcal{F}'_1 and of the lower envelope of \mathcal{F}'_2 is

$O((m+d)\lambda_4(k)/k)$, and any two continuous pieces, one from \mathcal{F}'_1 and one from \mathcal{F}'_2 , intersect each other in at most four points by Section 4. Thus, the number the combinatorial changes for the fixed contact pair is $O((m+d)\lambda_4(k)/k)$.

Consider the sum σ of the complexity $|\mathcal{F}'| = m$ of \mathcal{F}' over all classes for a fixed pair. Then the total sum of σ 's for all enumerations of fixed pairs is $O(k^3n^2)$ since $|\mathcal{T}| = O(k^3n^2)$. Similarly, consider the sum ξ of the number of intersections (d in the complexities in the previous paragraphs) over all classes for a fixed pair. Then the total sum of ξ 's for all enumerations of fixed pairs is $O(k^3n^2)$ since ξ is bounded by the number of combinatorial changes to eDT_θ for the convex hulls of three elements of P . Therefore, we conclude with the following theorem.

Theorem 11. *For a polygonal domain Q of size n and a convex k -gon P , the number of combinatorial changes to the edge Delaunay triangulation of Q under P_θ -distance for θ increasing from 0 to 2π is $O(k^2n^2\lambda_4(k))$.*

Theorem 11 directly improves the time complexity of the algorithm by Chew and Kedem.

Corollary 12. *Given a polygonal domain Q of size n and a convex k -gon P , we can find a largest similar copy of P that can be inscribed in Q in $O(k^2n^2\lambda_4(k)\log n)$ time using $O(kn)$ space.*

4 The number of critical orientations for four contact pairs

The orientation θ at which a combinatorial change to eDT_θ occurs is called a *critical orientation*. We consider the critical orientations θ at which \mathcal{P}_θ has contact with four contact pairs. We count the number of critical orientations for each (a, b) -change type. The number of critical orientations of $(0, 4)$ -change is 2, which is shown in Appendix B of [8]. So in this section, we count the critical orientations for the other types of combinatorial changes. The following table summarizes the results.

Types of (a, b) -change	(4, 0)	(3, 1)	(2, 2)	(1, 3)	(0, 4)
Number of critical orientations	1	2	4	2	2

4.1 Common intersection and directed angles

We need some technical lemmas before computing the critical orientations. For any two lines ℓ and ℓ' crossing each other in the plane, the *directed angle*, denoted by $\angle(\ell, \ell')$, is the angle from ℓ to ℓ' , measured counterclockwise around their intersection point. This definition can be extended for three points A, O , and B , and we use $\angle AOB = \angle(AO, BO)$ to denote the directed angle from the line through AO to the line through BO , measured counterclockwise around O . There are some properties of directed angles which we use in this section.

Proposition 13. *The following properties hold:*

1. *For any three points A, B , and O , we have $\angle AOB = -\angle BOA$ modulo π .*
2. *For any four points A, B, X , and Y such that no three of them are collinear, they are concyclic¹ if and only if $\angle XAY = \angle XBY$ modulo π .*
3. *For any three lines ℓ_1, ℓ_2 , and ℓ_3 such that no two lines are parallel, we have $\angle(\ell_1, \ell_2) + \angle(\ell_2, \ell_3) = \angle(\ell_1, \ell_3)$ modulo π . For any four points A, B, C , and O , we have $\angle AOB + \angle BOC = \angle AOC$ modulo π .*
4. *For any three lines ℓ_1, ℓ_2 , and ℓ_3 such that no two lines are parallel, we have $\angle(\ell_1, \ell_2) + \angle(\ell_2, \ell_3) + \angle(\ell_3, \ell_1) = 0$ modulo π .*

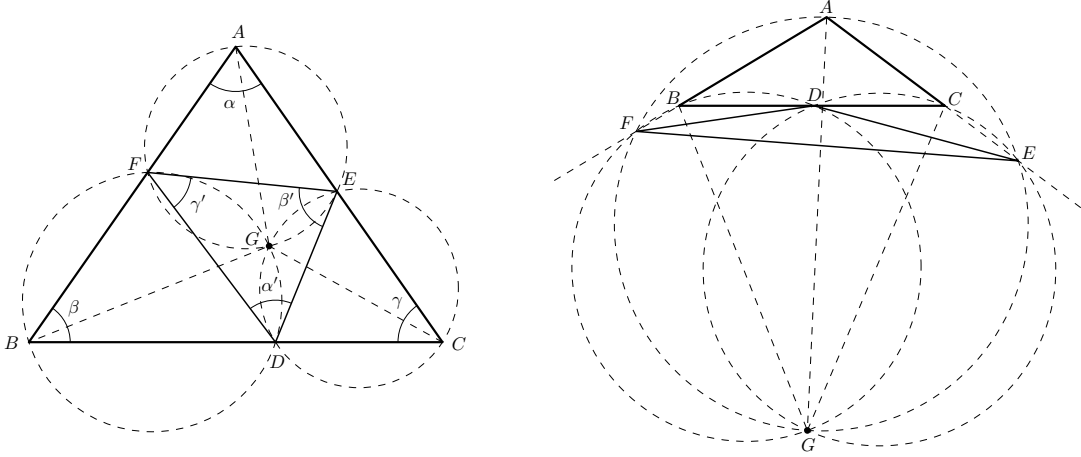


Figure 12: Some possible configurations of Lemmas 14 and 15.

See Figure 12 for an illustration of Lemmas 14 and 15.

Lemma 14 (Miquel's Theorem [9]). *Let $A, B,$ and C be the corners of a triangle, and let $D, E,$ and F be the points on the lines containing $CB, AC,$ and $AB,$ respectively. Then the three circumcircles to triangles EAF, FBD and DCE have a common point of intersection.*

Lemma 15. *Let $A, B,$ and C be the corners of a triangle, and let $D, E,$ and F be the points on the lines containing $CB, AC,$ and $AB,$ respectively. Let G be the intersection of three circumcircles to triangles EAF, FBD and $DCE,$ and let $\angle BAC = \alpha, \angle CBA = \beta, \angle ACB = \gamma, \angle EDF = \alpha', \angle FED = \beta', \angle DFE = \gamma'$ modulo π for fixed angles $\alpha, \beta, \gamma, \alpha', \beta',$ and γ' .*

1. $\angle AGB = \gamma - \alpha' - \beta', \angle BGC = \alpha - \beta' - \gamma',$ and $\angle CGA = \beta - \gamma' - \alpha'$ modulo $\pi,$ regardless of $\angle EFA.$
2. If ABC or DEF remains unchanged while $\angle EFA$ is changing, G remains unchanged.
3. $\angle GDF, \angle EDG, \angle GED, \angle FEG, \angle GFE,$ and $\angle DFG$ remain unchanged while $\angle EFA$ is changing.

Proof. See Figure 12 for an illustration.

1. Suppose that $\angle GDF = \alpha_1, \angle EDG = \alpha_2, \angle GED = \beta_1, \angle FEG = \beta_2, \angle GFE = \gamma_1,$ and $\angle DFG = \gamma_2$ modulo $\pi.$ Then,

$$\begin{aligned} \alpha &= \beta_2 + \gamma_1, & \beta &= \gamma_2 + \alpha_1, & \gamma &= \alpha_2 + \beta_1, & & \text{(by Proposition 13.2)} \\ \alpha' &= \alpha_1 + \alpha_2, & \beta' &= \beta_1 + \beta_2, & \gamma' &= \gamma_1 + \gamma_2 \end{aligned}$$

modulo $\pi.$ Using the equations above, we have

$$\begin{aligned} \angle AGB &= -\angle GBA - \angle BAG = -\angle GBF - \angle FAG = -\angle GDF - \angle FEG \\ &= -\alpha_1 - \beta_2 = \gamma - \alpha' - \beta' \end{aligned}$$

modulo $\pi.$ We can show $\angle BGC = \alpha - \beta' - \gamma',$ and $\angle CGA = \beta - \gamma' - \alpha'$ modulo π in the same way.

¹A set of points are said to be *conyclic* if they lie on a common circle.

2. Suppose that triangle ABC remain unchanged while $\angle EFA$ is changing. By Lemma 15.1, the circumcircles to triangles ABG , BCG , and CAG remain unchanged. Thus, their common intersection G also remains unchanged. When the triangle DEF remains unchanged, G also remains unchanged since the circumcircles to triangles EAF , FBD , and DCE remain unchanged.
3. It is deduced by Lemma 15.2. □

4.2 Counting critical orientations

Now we count the critical orientations which is induced by the same set of contact pairs. To do this, we count the orientations θ at which \mathcal{P}_θ satisfies the four contact pairs, $C_i = (A_i, B_i)$ for $i = 1, \dots, 4$. We consider each type of (a, b) -changes in the following.

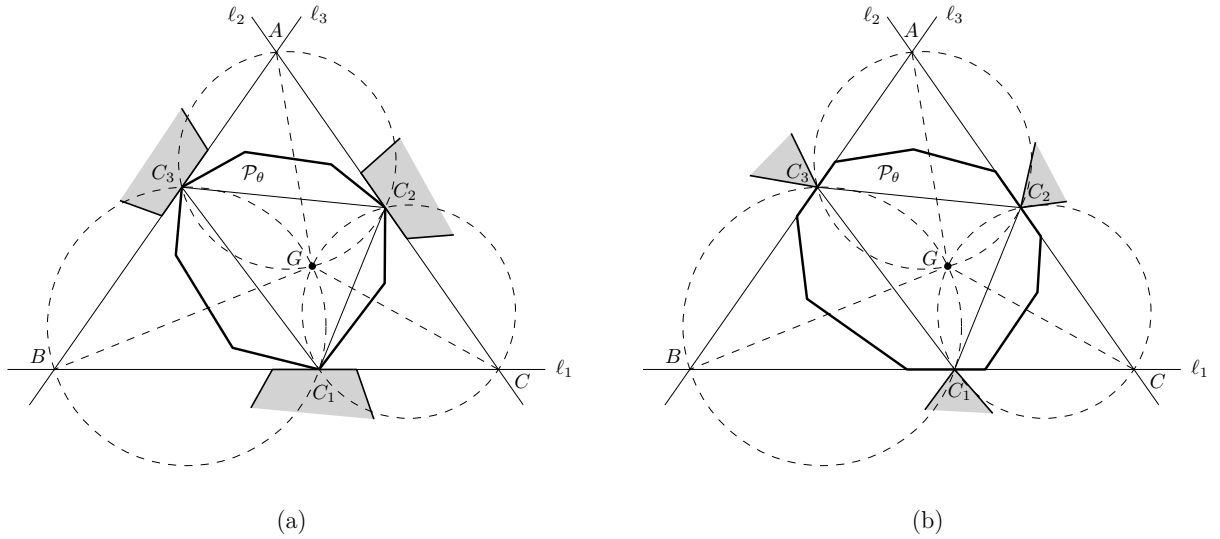


Figure 13: (a) \mathcal{P}_θ satisfies the side contact pairs $C_i = (A_i, B_i)$ for $i = 1, 2, 3$. (b) \mathcal{P}_θ satisfies the corner contact pairs $C_i = (A_i, B_i)$ for $i = 1, 2, 3$.

(4, 0)-changes and (3, 1)-changes. Suppose that C_1, C_2 , and C_3 are side contact pairs and \mathcal{P}_θ satisfies them. Let ℓ_i be the line through A_i for each $i = 1, 2, 3$, and let $A = \ell_2 \cap \ell_3$, $B = \ell_1 \cap \ell_3$, and $C = \ell_1 \cap \ell_2$. By Lemma 14, the circumcircles to triangles AB_2B_3 , BB_3B_1 , and CB_1B_2 have a common intersection point, denoted by G . See Figure 13(a). By Lemma 15.2, G remains unchanged for any θ since A, B , and C remain unchanged. Also, $\angle B_2B_1G$ and $\angle GB_2B_1$ remain unchanged by Lemma 15.3.

We use \overrightarrow{XY} to denote the vector from point X to point Y . Let $\Phi_{s, \vartheta}$ denote the affine transformation with scale factor s and rotation angle ϑ in counterclockwise direction. Then there exist s and ϑ such that $\overrightarrow{GB_2} = \Phi_{s, \vartheta} \overrightarrow{GB_1}$ for every \mathcal{P}_θ satisfying C_1, C_2 , and C_3 . For a vertex V of \mathcal{P} , $\overrightarrow{GV} = t_1 \overrightarrow{GB_1} + t_2 \overrightarrow{GB_2}$ for constants t_1 and t_2 . Therefore, $\overrightarrow{GV} = \Phi_{s', \vartheta'} \overrightarrow{GB_1}$ for some s' and ϑ' , and the trace of V is a line segment.

If C_4 is also a side contact pair, the traces of B_4 and A_4 intersect each other at most once since the trace of B_4 is a line segment. Therefore, there is at most one critical orientation for a $(4, 0)$ -change. Consider the case that C_4 is a corner contact pair. Assume that $B_4 = V_1V_2$,

for vertices V_1 and V_2 of P . Since the trace of V_1 is a segment, $\overrightarrow{GV_1}$ can be parametrized to $t\vec{v}_1 + \vec{c}_1$ for some \vec{v}_1, \vec{c}_1 and $t = t(\theta)$. Since $GV_2 = \Phi_{s_1, \vartheta_1} \overrightarrow{GV_1}$ for some s_1 and ϑ_1 , $\overrightarrow{GV_2}$ can be parametrized to $t\vec{v}_2 + \vec{c}_2$ for some \vec{v}_2, \vec{c}_2 and $t = t(\theta)$. If \mathcal{P}_θ satisfies C_4 , we have $\overrightarrow{GA_4} = t'\overrightarrow{GV_1} + (1-t')\overrightarrow{GV_2} = t't(\vec{v}_1 - \vec{v}_2) + t'(\vec{c}_1 - \vec{c}_2) + t\vec{v}_2 + \vec{c}_2$ for some t and $t' \in [0, 1]$. Thus, we obtain two equations for t' and t in x - and y -coordinates. By eliminating t' using these two equations, we obtain a quadratic equation for t which has at most two solutions. Therefore, there are at most two critical orientations for a $(3, 1)$ -change.

(1, 3)-changes. Suppose that C_1, C_2 , and C_3 are corner contact pairs and C_4 is a side contact pair. Let \mathcal{P}_θ satisfies these three corner contact pairs. Let ℓ_i be the lines through B_i for each $i = 1, 2, 3$, and let $A = \ell_2 \cap \ell_3, B = \ell_1 \cap \ell_3$, and $C = \ell_1 \cap \ell_2$. By Lemma 14, the circumcircles to triangles AA_2A_3, BA_3A_1 , and CA_1A_2 have a common intersection point G . See Figure 13(b). By Lemma 15.2, G remains unchanged while θ increases since A_1, A_2 , and A_3 remain unchanged. Also, $\angle ABG$ and $\angle GAB$ remain unchanged by Lemma 15.3. Therefore, $\overrightarrow{GB} = \Phi_{s, \vartheta} \overrightarrow{GA}$ for some s and ϑ . Then, $\overrightarrow{GB_4} = t_1 \overrightarrow{GA} + t_2 \overrightarrow{GB}$ for constants t_1 and t_2 . Therefore, $\overrightarrow{GB_4} = \Phi_{s', \vartheta'} \overrightarrow{GA}$ for some s' and ϑ' , and the trace of B_4 is an arc of a circle through G . Since the traces of B_4 and A_4 intersect each other in at most two points, there are at most two critical orientations for a $(1, 3)$ -change.

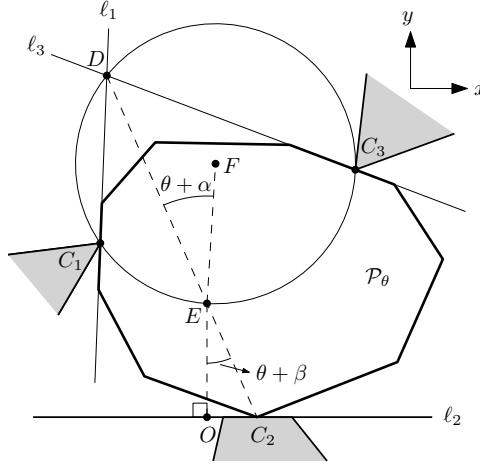


Figure 14: \mathcal{P}_θ satisfies the contact pairs $C_i = (A_i, B_i)$ for $i = 1, 2, 3$.

(2, 2)-changes. Suppose that C_1 and C_3 are corner contact pairs and C_2 and C_4 are side contact pairs, and \mathcal{P}_θ satisfies C_1, C_2 , and C_3 . Let ℓ_1, ℓ_2 , and ℓ_3 be the lines through B_1, A_2 , and B_3 , respectively, and let $D = \ell_1 \cap \ell_3$. Let F be the center of the circumcircle to triangle A_1A_3D , and let E be the intersection of the circumcircle and B_2D , other than D . Let O be the perpendicular foot of E to ℓ_2 . Let $\theta + \alpha$ be the angle from \overrightarrow{EF} to \overrightarrow{ED} and $\theta + \beta$ be the angle from \overrightarrow{EO} to $\overrightarrow{EB_2}$ counterclockwise. See Figure 14. Since the angle between $\overrightarrow{DA_1}$ and $\overrightarrow{DB_2}$ remains unchanged while θ increases, E, F and O remain unchanged. We have $\overrightarrow{B_2B_4} = \Phi_{s, \vartheta} \overrightarrow{B_2D}$ for some s and ϑ . We also have $\overrightarrow{OB_4} = \overrightarrow{OB_2} + \overrightarrow{B_2B_4} = \overrightarrow{OB_2} + \Phi_{s, \vartheta} \overrightarrow{B_2D} = (|EO| \tan(\theta + \beta), 0) + \Phi_{s, \vartheta} (|EO| \tan(\theta + \beta) - 2|EF| \cos(\theta + \alpha) \sin(\theta + \beta), |EO| + 2|EF| \cos(\theta + \alpha) \cos(\theta + \beta))$. Observe that each point V on segment A_4 can be parametrized to $\overrightarrow{OV} = s\vec{v} + \vec{c}$ for some \vec{v} and \vec{c} . If B_4 touches A_4 , then $s\vec{v} + \vec{c} = \overrightarrow{OB_4}$ is satisfied for some s . Thus, we obtain two equations for θ and s in x - and y -coordinates. By eliminating s using these two equations, we obtain the equation for θ . By

substituting $t = \tan \frac{\theta+\beta}{2}$, we obtain a quartic equation for t which has at most four solutions. Therefore, there are at most four critical orientations for a $(2, 2)$ -change.

References

- [1] Pankaj K Agarwal, Nina Amenta, and Micha Sharir. Largest placement of one convex polygon inside another. *Discrete & Computational Geometry*, 19(1):95–104, 1998.
- [2] Pankaj K Agarwal, Boris Aronov, and Micha Sharir. Motion planning for a convex polygon in a polygonal environment. *Discrete & Computational Geometry*, 22(2):201–221, 1999.
- [3] Mikhail J Atallah. Dynamic computational geometry. In *Proceedings of the 24th Annual Symposium on Foundations of Computer Science (FOCS 1983)*, pages 92–99. IEEE, 1983.
- [4] Francis Avnaim and Jean Daniel Boissonnat. Polygon placement under translation and rotation. In Robert Cori and Martin Wirsing, editors, *STACS 88*, pages 322–333. Springer Berlin Heidelberg, 1988.
- [5] Sang Won Bae and Sang Duk Yoon. Empty squares in arbitrary orientation among points. In *Proceedings of the 36th International Symposium on Computational Geometry (SoCG 2020)*. Schloss Dagstuhl-Leibniz-Zentrum für Informatik, 2020.
- [6] Bernard Chazelle. The polygon containment problem. In F.P. Preparata, editor, *Advances in Computing Research, Vol I: Computational Geometry*, pages 1–33. JAI Press Inc., 1983.
- [7] L Paul Chew and Klara Kedem. Placing the largest similar copy of a convex polygon among polygonal obstacles. In *Proceedings of the 5th Annual Symposium on Computational Geometry (SoCG 1989)*, pages 167–173, 1989.
- [8] L Paul Chew and Klara Kedem. A convex polygon among polygonal obstacles: Placement and high-clearance motion. *Computational Geometry*, 3(2):59–89, 1993.
- [9] Harold Scott Macdonald Coxeter and Samuel L Greitzer. *Geometry revisited*, volume 19. The Mathematical Association of America, 1967.
- [10] Rudolf Fleischer, Kurt Mehlhorn, Günter Rote, Emo Welzl, and Chee Yap. Simultaneous inner and outer approximation of shapes. *Algorithmica*, 8(1):365, 1992.
- [11] Steven Fortune. A fast algorithm for polygon containment by translation. In *Proceedings of the 12th International Colloquium on Automata, Languages, and Programming (ICALP 1985)*, pages 189–198. Springer, 1985.
- [12] Jacob E. Goodman, Joseph O’Rourke, and Csaba D. Tóth, editors. *Handbook of Discrete and Computational Geometry*. CRC Press LLC, 3rd edition, 2017.
- [13] Daniel P Huttenlocher, Klara Kedem, and Jon M Kleinberg. On dynamic Voronoi diagrams and the minimum Hausdorff distance for point sets under Euclidean motion in the plane. In *Proceedings of the 8th Annual Symposium on Computational Geometry (SoCG 1992)*, pages 110–119, 1992.
- [14] Klara Kedem and Micha Sharir. An efficient motion-planning algorithm for a convex polygonal object in two-dimensional polygonal space. *Discrete & Computational Geometry*, 5:43–75, 1990.

- [15] Seungjun Lee, Taekang Eom, and Hee-Kap Ahn. Largest triangles in a polygon. *arXiv preprint arXiv:2007.12330*, 2020.
- [16] Daniel Leven and Micha Sharir. Planning a purely translational motion for a convex object in two-dimensional space using generalized voronoi diagrams. *Discrete & Computational Geometry*, 2:9–31, 1987.
- [17] Nimrod Megiddo. Applying parallel computation algorithms in the design of serial algorithms. *Journal of the ACM*, 30(4):852–865, 1983.
- [18] Colm Ó’Dúnlaing and Chee K Yap. A retraction method for planning the motion of a disc. *Journal of Algorithms*, 6(1):104–111, 1985.
- [19] Micha Sharir and Sivan Toledo. Extremal polygon containment problems. *Computational Geometry*, 4(2):99–118, 1994.
- [20] Endre Szemerédi. On a problem by davenport and schinzel. *Acta Arithmetica*, 25:213–224, 1974.
- [21] Sivan Toledo. Extremal polygon containment problems. In *Proceedings of the 7th Annual Symposium on Computational Geometry (SoCG 1991)*, pages 176–185. ACM, 1991.